HEMATITE SPHERULES AT MERIDIANI: RESULTS FROM MI, MINI-TES AND PANCAM. W. M. Calvin[1], J. D. Shoffner[1], J. M. Pocock[1], J. R. Johnson[2], A. T. Knudson[3], D. Rogers[4], T. D. Glotch[4], S. W. Ruff[5], [1]Dept. Geological Sciences and Engineering, University of Nevada, Reno, NV 89557 (wcalvin@unr.edu) [2]Astrogeology Team, U. S. Geological Survey, [3]Dept. Earth and Planetary Sciences, Washington University, [4]Dept. Geological Sciences, CalTech, [5]Dept. Geological Sciences, Arizona State University.

Introduction: Among the interesting surprises at the Mars Exploration Rover Opportunity landing site was the observation that the signature of bulk hematite observed by the MGS Thermal Emission Spectrometer (TES) on orbit was caused by small rounded grains on surface. Initial analysis showed that the infrared spectral signature was absent in airbag bounce marks where the spheres were depressed into the surface and Pancam spectra of undisturbed soils showed a 900 nm absorption consistent with coarse grey hematite. The Alpha-Particle X-ray Spectrometer (APXS) showed strong elemental lines of iron and M_ssbauer Spectrometer (MB) data show the characteristic Fe^{3+} sextet associated with hematite [1-4].

More detailed analysis confirmed the hematite contribution in numerous soils and in small grains armoring dune crests [5], that the infrared signature of hematite appears as an isolated spectral endmember in spectral transformations [6], but the bulk composition as determined by APXS suggests that there may be a silicate contribution to these spheres and they may not be pure Fe_2O_3 [7]. More recent work suggests that a thin coating of dust may have the same effect as a non-hematite component on the APXS spectra [8]. Based on the uniformity in size, the dispersed distribution of the spheres in outcrop, lack of concentration along bedding planes, rare doublets and raised bedding plane ridges, the spheres are interpreted to be post-depositional diagenetic concretions [7]. This interpretation is supported by the size variations seen in the long traverse to Victoria crater and attributed to variation in fluid flow regimes [9].

Our work synthesizes observations of the spheres using Microscopic Imager (MI), Pancam and the Mini-Thermal Emission Spectrometer (Mini-TES). Observations made in the first 950 sols of Opportunity's landed explorations include systematic coordinated observation using both Pancam and Mini-TES, Rock Abrasion Tool (RAT) grinds in outcrop, and directional Mini-TES scans across the plains. These observations were designed to constrain interior structure, formation mechanisms and history for the spheres.

Size and Frequency from MI: The spheres are ubiquitous and between Eagle and Endurance were remarkably even in size and tone [10]. Grains were observed to be spherical to subspherical with a median diameter of roughly 4mm. The size of the spherules was noted to shrink, and they became more prevalent in outcrop beginning near Vostok crater (Figure 1). In the "One Scoop" target just north of Erebus dark irregular patches are seen in the RAT hole, and the darkest of these are mostly spherical and interpreted as spherules (Figure 2). In the outcrop target "Baltra" at Beagle crater well formed but very small spheres are again seen. (Figure 3).

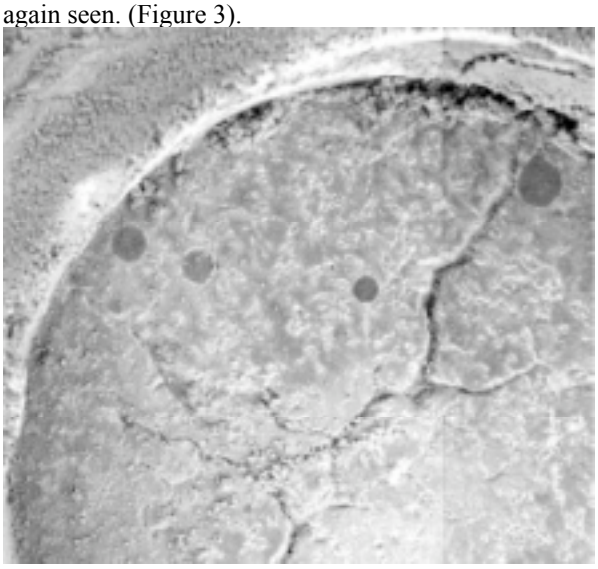

Figure 1. Gagarin at Vostok Sol 403.

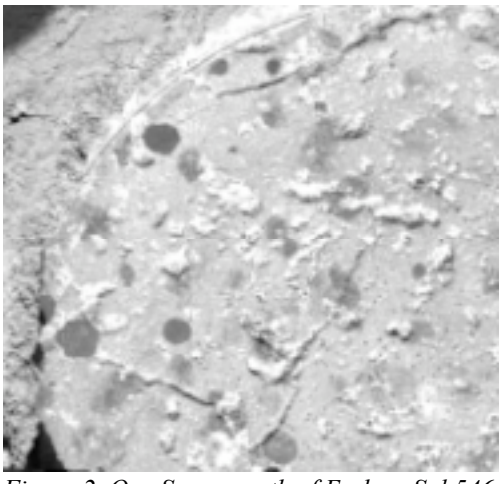

Figure 2. One Scoop north of Erebus, Sol 546.

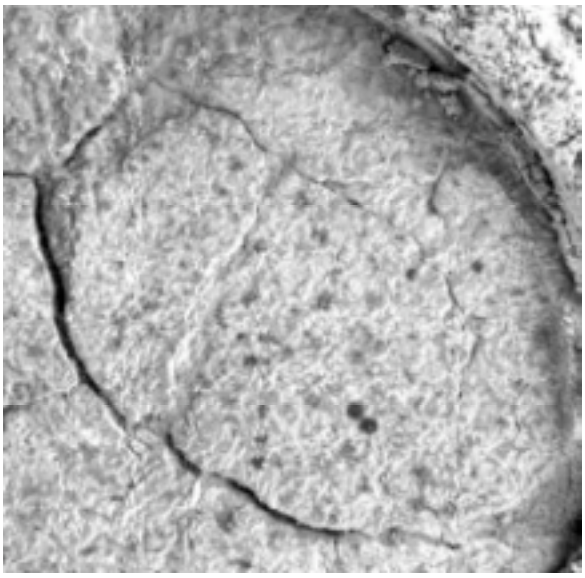

Figure 3. Very small spheres in Baltra, Sol 894.

Opportunity performed 25 RAT grind operations in outcrop and sliced through approximately 70 individual spherules. The appearance after ratting shows no interior structure at the spatial scale of MI (30 μm/pixel) and they remain uniformly grey in color. They can preserve scratches from the grinding wheel or become dislodged by ratting, indicating they are harder than the host rock. In one instance a potential fracture was identified in a Ratted rock, and fractured spheres are seen loose on the plains.

Summary of Properties

- Dominantly spherical or sub-spherical. Some are split, and rare angular or irregular shapes.
- Appear loose on top of outcrop materials, plains units, and crater interiors.
- Appear in various stages of erosion from within outcrop materials.
- Cross layers within finely bedded sedimentary structures. Are split by fractures in surrounding host rock. Are not aggregated along bedding planes.
- Occur primarily as single spheres, but occasionally appear double or fused.
- Occasional presence of latitudinal grooves or ridges.
- Smooth surfaces but sometimes "orange skin" texture is seen.
- Surrounding sediment is more coarsely crystalline than in the outcrops in general.
- In Endurance and near the rim of Victoria outcrop coated spheres were observed.
- Grade in size south of Endurance (up section) from ~ 4mm to <1mm, the size that is also seen armoring ripple crests.

Coordinated Pancam and Mini-TES: Sixty coordinated Pancam and Mini-TES observations were made of soils in the near field between sols 70 and 800. These are low elevation closely-spaced Mini-TES rasters or stares, allowing comparison of distant emission variations with local scale changes in soil signatures and comparison of imaging with infrared features. These data were acquired periodically in the traverse from Eagle across to Endurance then south toward Victoria crater. We selected 15 observations that had both full 13 filter Pancam coverage and high quality Mini-TES spectra of homogenous soils (e.g. Figure 4). We determined a "hematite strength" index using the band depth of the infrared absorptions in Mini-TES and a color ratio index in Pancam.

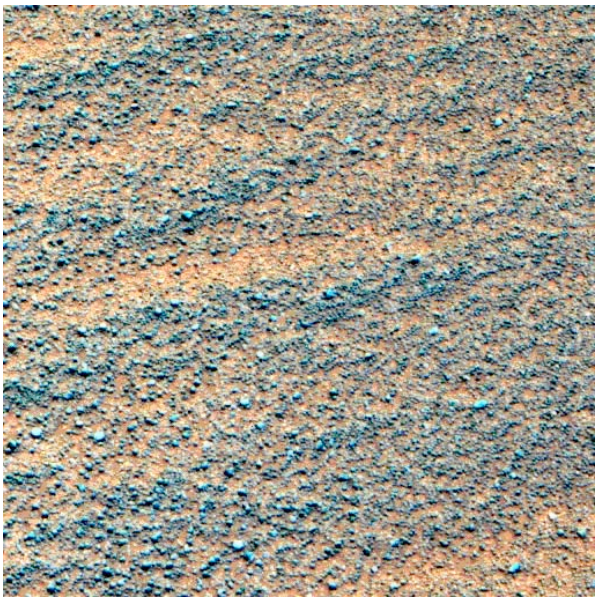

Fig. 4: Pancam Systematic Foreground image (sequence P2563, Sol 518) created from L2 (753 nm), L5 (535 nm), and L7 (432 nm) filters.

Mini-TES Methods: Over the course of the mission, dust has accumulated on the Mini-TES mirror. This creates a large, broad absorption feature in calibrated emissivity spectra of the soils. For the majority of the mission, this signature has not impacted the lower wavenumbers (longer wavelengths) where the hematite features occur. However, this contribution has worsened over time and in later sols a very strong dust signature will also affect the hematite wavelengths. To determine the hematite abundance we have explored two methods. The first corrects for the mirror dust and

then determines a hematite band depth using the shoulder at 750 cm^{-1} and the depth at 550 cm^{-1}. The second method determines a hematite "index" on uncorrected emissivity spectra. The index is the sum of the two band depths at 550cm^{-1} and 450 cm^{-1} relative to the peak height at 500cm^{-1} (A-B)+(A-C), where A is the emissivity at the peak and B and C are values at the band centers. The two methods correlate extremely well and we prefer the dust-corrected index in most instances, except when the dust signature is very low. Figure 5 shows the dust corrected spectra. While there is variability in the strength of the hematite index seen in the traverse from Endurance to Victoria, the Mini-TES hematite index does not correlate well with the decreasing size observed with MI. That is, regardless of sphere size the area covered is reasonably uniform in the soil lag.

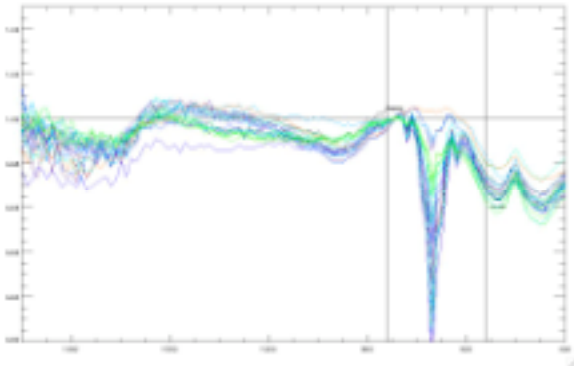

Figure 5: Dust-corrected Mini-TES of systematic soils. Hematite index is determined using the band shoulder and band center shown as horizontal black bars.

Pancam Methods: In order to best estimate the fractional area covered by "blueberries" in each Pancam scene we restricted our analysis to those images with all 13 filters. We explored a number of classification schemes including unsupervised classification of either left or right eye filters, band ratios, relative band depths and band slopes as shown by Farrand et al. [11] to be useful for discriminating spheres against the background soil. The methods that performed best were either a decorrelation stretch (DCS) of right eye filters or a thresholded band ratio. The first method performs a DCS using right-eye filters R3,2,1. The blud band of the DCS is then ratioed to R6/R7. The second method uses the R1/R2 ratio in a simple color composite (Red-Green-Blue) with R1 (G) and R6/R7 (B). However, fairly large uncertainties exist for the Pancam area index due to shadowing at the edge of spheres, illumination gradation across the scene, misclassification of dust covered berries as soil, and issues associated with ripples in images. Early methods also misclassified basaltic cobbles as berries and led us to a supervised method where endmembers are selected from the DCS method. Using a limited set of Pancam images where we believe the supervised classification schemes work well there is reasonable correlation between the Mini-TES index and the Pancam fractional area covered showing that these two methods are seeing the same component of the soils.

Directional Emissivity with Mini-TES: Plains scans were obtained inside Eagle crater, where Opportunity was below the local plains level, just outside of Eagle, in the vicinity of the Heatshield, south of Endurance, and a series of dune face observations were made beginning with Purgatory, the ripple in which Opportunity temporarily got stuck in June 2005. We concentrate on those plains scans occurring outside Eagle crater (Sols 57-72), and in the vicinity of the heatshield (Sols 354-372). In both cases the rover was on fairly level terrain so that the instrument elevation angle can be used to determine an approximate surface emission angle through simple geometry. The data cover a wide variety of azimuth and generally observe from near the rover to the horizon over homogenous terrain.

Hematite Band Strength Variability: There is a strong and consistent pattern of increasing band strength with larger emission angles (smaller instrument elevation angle) on the plains (Figure 6). It should be noted that while the hematite features are observed to increase significantly, there is no associated increase in band strength in the 10-μm region. This observation suggests, that at least to Mini-TES, the composition of the spheres is dominated by hematite and not any potential silicate component. This is consistent with the conclusion from the MB spectrometer [5], although that instrument is only sensitive to iron-bearing components.

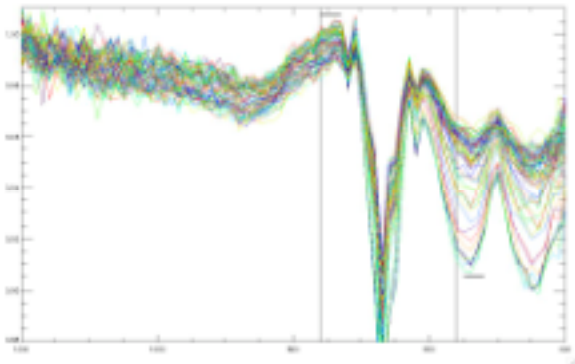

Figure 6: Increase in hematite band strength with distance on the plains.

Observations from different Sols and locations all show the same elevation angle dependence (Figure 7). Small deviations throughout can be accounted for by heterogeneity in berry cover, varying dune face geometry, noise levels in the early, low-sum scans and the extreme distances involved in the smallest elevation angle observations. The highly variable foreground observations also cluster around the trend observed from the vertical scans at the lowest elevation angles. The increase in projected area of the Mini-TES spot size is predicted to follow a $(1/\cos(q))^3$ curve, where q is the complement of the elevation angle. This approximate fit is shown as the dashed line. While this measure works well nearest the rover, the observations deviate from this simple geometrical relationship at elevations above -15 degrees.

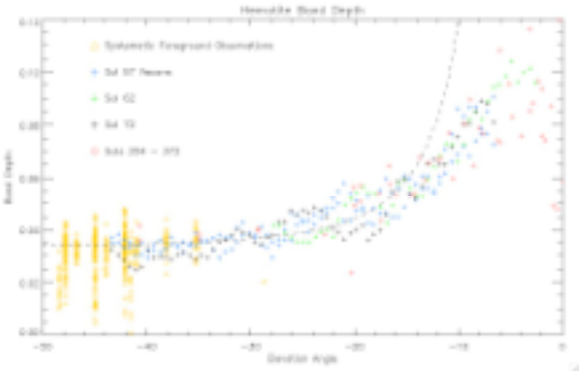

Figure 7: Hematite index with elevation angle or directional increase in band strength with increased emission angle.

The lack of a feature at 390 cm^{-1} in the spectra from TES in orbit and Mini-TES on the surface suggests that the emission is dominated by a single crystal axis (c-face), as can occur if the crystal grains are oriented (laminated or platy structure). Recent work by Glotch et al. [12] models spectra from spherules using Fresnel refelctance theory and notes that either random thin plates or interior concentric laminations could account for the observed spectra. Radial needle orientation could also account for the observed spectra. We note that in all of the Fresnel models band center shifts and relative changes in band strength are observed at emission angles of 75 degrees – the same point at which the directional emissivity variation deviates from a simple geometric curve. Recent work by Pitman [13] also suggests that emissivity band strength increases at higher emission angles.

Summary: The visual appearance of the spheres and gradation in size south of Endurance suggest either a changing depositional environment or variation in the duration and timing of diagenetic events as Opportunity moved up-section in the sedimentary sequence. Coated grains seen in Endurance and at the target Cha, just outside of Victoria support the complex diagenetic history espoused by McLennan et al. [7]. While diversity is seen in the size and appearance of berries in outcrop, the soil lag is fairly uniform, at least in terms of a hematite index derived from either Pancam or Mini-TES. Neither MI nor Mini-TES offer much constraint on interior structure, though the lack of a 390 cm^{-1} feature suggest interior concentric or radial structure at scales too fine for MI to observe. Mini-TES does not see any component other than hematite in the composition of the spheres. The dominant size population observed early in the mission in ripple crests is observed as the primary population in ratted outcrop farther south. This suggests that the overlying sediments that have eroded to leave the present lag deposit had a population of smaller spheres in addition to the orginal size distribution seen in Eagle and Endurance. This also suggests the spheres are more resistant to fracture, abrasion and size reduction than was originally thought. It will be interesting, if Opportunity ventures into Victoria crater, to see if the population gets larger in the sequence lower than what we have observed so far.

References: [1] Squyres, S. W., et al. (2006) JGR, 111, doi:10.1029/2006JE002771. [2]Christensen, P. R., et al., (2004) Science, 306, p.1733. [3]Bell, J.F. III, et al., (2004) Science, 306, p. 1703. [4]Rieder, R. et al.(2004) Science, 306, p. 1746. [5]Morris et al., (2006) JGR, 111, doi:10.1029/2006JE002791 [6]Glotch, T. D., and J. L. Bandfield (2006) JGR-Planets, 111, doi:10.1029/2005JE002671. [7]McLennan, S. M., et al. (2005) EPSL, 240, 95-121, [8]Jolliff et al. (2007) LPSC XXXVIII, abs.#2279; and this conference. [9]Squyres, S. W., et al. (2006) Science, 313, p. 1403. [10] Weitz et al. (2006) JGR, 111, doi:10.1029/2005JE002541. [11]Farrand W. H. et al. submitted. [12]Glotch, T. D., et al. (2006), Icarus, 181, p. 408 [13]Pitman, K.M. et al. (2006) LPSC XXXVII, abs.#1336.

Acknowledgements: This work is supported by the Mars Exploration Project Participating Scientist grant to Calvin with additional sponsorship from Nevada Space Grant and EPSCoR programs. We appreciate the sustained, dedicated participation of the Athena Science team and JPL engineering staff in continued operation and science observations of Spirit and Opportunity.